Journal of Russian Laser Research, Volume 21, Number 1, 2000

WAVEGUIDE SPECTRAL MULTIPLEXERS/DEMULTIPLEXERS

T. K. Chekhlova and I. V. Tcheremiskin

Russian People's Friendship University, Department of Radiophysics, Ul. Miklukho-Maklaya 6, Moscow 117198, Russia

e-mail: itcheremiskin@sci.pfu.edu.ru tchekhlova@sci.pfu.edu.ru

Abstract

Configurations, basic characteristics, and the methods for implementation of wavelength-division multiplexers/demultiplexers as the key elements of the end stations in fiber-optics communication systems are considered. The most important studies directed at practical implementation of wavelength-division multiplexers in specific devices based on SiO_2 and InP are reviewed in detail. SiO_2-based multiplexers exhibit lower losses, whereas devices based on InP make it possible to use the technologies of microelectronics and integrating optics and to fabricate radiation sources and passive components on the same substrate. Schemes for optical multiplexers with adding and dropping of channels and examples of their implementation are given. It is emphasized that high-density wavelength-division multiplexers have small sizes and are fabricated by conventional lithography, which makes them promising in wideband optical communication systems.

1. Introduction

The intensive development of fiber-optics (FO) communication systems and the possibility of transmitting large data flows through an FO waveguide pose the problem of using to full advantage the entire passband of an FO waveguide. At the early stage of development of FO communication systems, the possibility of wide-band communication lines based on a single optical carrier with time-dividing channeling was considered. In this case, the bandwidth of transmitted frequencies was found to be limited by dispersion phenomena in the fiber and amounted to a negligible fraction of the passband of the FO waveguide. Later on, various methods for spectral multiplexing (demultiplexing) of optical channels were developed [1, 2]. Separation of channels was accomplished with the use of various dispersive components; most often, planar diffraction gratings were used. In a number of studies [3–6], waveguide spectral analyzers of the Michelson echelon were used as waveguide spectral multiplexers; such an analyzer is, in fact, a waveguide phase grating with a relatively small number of interfering rays and a large constant phase difference between neighboring rays. In the available publications, there are a number of terms used for the above systems for the frequency-division multiplexing/demultiplexing in the waveguide integrated circuits: a waveguide spectral analyzer (WSA) of the Michelson echelon type, a waveguide spectral multiplexer/demultiplexer [or wavelength-division multiplexer/demultiplexer (WDM/D)], and a spectral multiplexer/demultiplexer based on arrays of phased waveguides (PHASAR, AWG, and AWR). Conceptually, all the mentioned systems belong to the same class with minor structural differences. Therefore, in what follows, we will use the terms adopted from the cited papers.

Recently, as can be judged from numerous publications, the WDM/D are the most promising systems for multiplexing the channels because these systems make it possible to use the entire passband of an FO waveguide for communication purposes. Furthermore, a merit of WDM consists in the possibility of implementing them with the use of the well-known and well-developed technologies of microelectronics and integrated optics, which makes it possible to integrate optical and electronic components in the same chip and also ensure a

Translated from a manuscript submitted September 23, 1999.

1071-2836/00/2101-0081$25.00

connection to an FO waveguide. The FO waveguide systems are fabricated by photolithography and do not present any unresolvable problems in mass production.

Modern development of FO communication systems, theoretical and experimental studies of WDM, and technological potentials of their fabrication make it possible to pass from the problem of FO communication line by large distances (continent-to-continent and town-to-town) to the solution of problems of intercity communication lines inclusive of building-to-building lines. In this case, it turns out that, with allowance made for the progress in computer techniques, there is an increase in the requirement for the use of increasingly larger databases, the necessity of varying these data in real time, and so on. Correspondingly, an expansion of the frequency range is also required. The key to the solution of the aforementioned problems is the wide use of WDM in the output stages of FO communication lines. According to the review of available publications, the scientific and technological base for the industrial use of WDM/D has basically been established.

2. Basic Schemes and Fundamental Characteristics

The first suggested schemes of WDM/Ds and WSAs were conceptually the different variants of the known spectral device – the Michelson echelon [3–9]. The differences between them were largely related to the method of their implementation and the domain of applicability. The formulas defining the basic characteristics of WDM/D and WSA are virtually similar in view of the reversibility principle, and they can be derived by analogy with the derivation of bulk Michelson echelons [10] with allowance made for the fact that the optical beams propagate along the planar (channeling) waveguides or fiber-optics waveguides. Figure 1 shows the schemes of disperse WSA systems of transparent type (a), of WDM based on channeling waveguides (b), and of WSA based on fiber-optics waveguides (c). The formulas defining the basic characteristics of WDM and WSA fabricated on the basis of single-mode waveguides are written as

$$
\begin{aligned}
D_\varphi = \frac{h}{\gamma X_0 \lambda} b, \quad \mathcal{R} = \frac{Nh}{\lambda} b, \quad \Delta\lambda = \frac{\lambda^2}{hb}, \\
\Delta\varphi = \frac{\lambda}{\gamma X_0}, \quad \delta\lambda = \frac{\lambda^2}{Nhb}, \quad \delta\varphi = \frac{\lambda}{N\gamma X_0}, \\
b = \Delta\gamma - \lambda \frac{d\Delta\gamma}{d\lambda}, \quad \Delta\gamma = \gamma_1 - \gamma_2, \quad K = \frac{\Delta\gamma h}{\lambda}.
\end{aligned}
\tag{1}
$$

In formulas (1), the following notations are used:
D_φ as angular dispersion,
$\mathcal{R}$ as resolution,
$\Delta\lambda$ as spectral range of dispersion,
$\Delta\varphi$ as the angular interval between the neighboring orders of the spectrum,
$\delta\lambda$ and $\delta\varphi$ as minimum distance and minimum angle between the lines Rayleigh resolved,
b as dispersion factor,
h as constant path difference between the adjoining stages (waveguides),
X_0 as width of the stages (channels),
γ_1 and γ_2 as effective refractive indices of the steplike structure and the operative waveguide,
λ as the wavelength in vacuum,
N as number of interfering rays (channels),
K as the spectrum order.

For waveguide multiplexers based on channel waveguides and FO waveguides (Fig. 1b and 1c), the difference $\Delta\gamma$ in the above formulas should be changed to the value of the effective refractive index of the corresponding waveguide. In addition, in the case of a reflective WSA, doubling of the optical path length

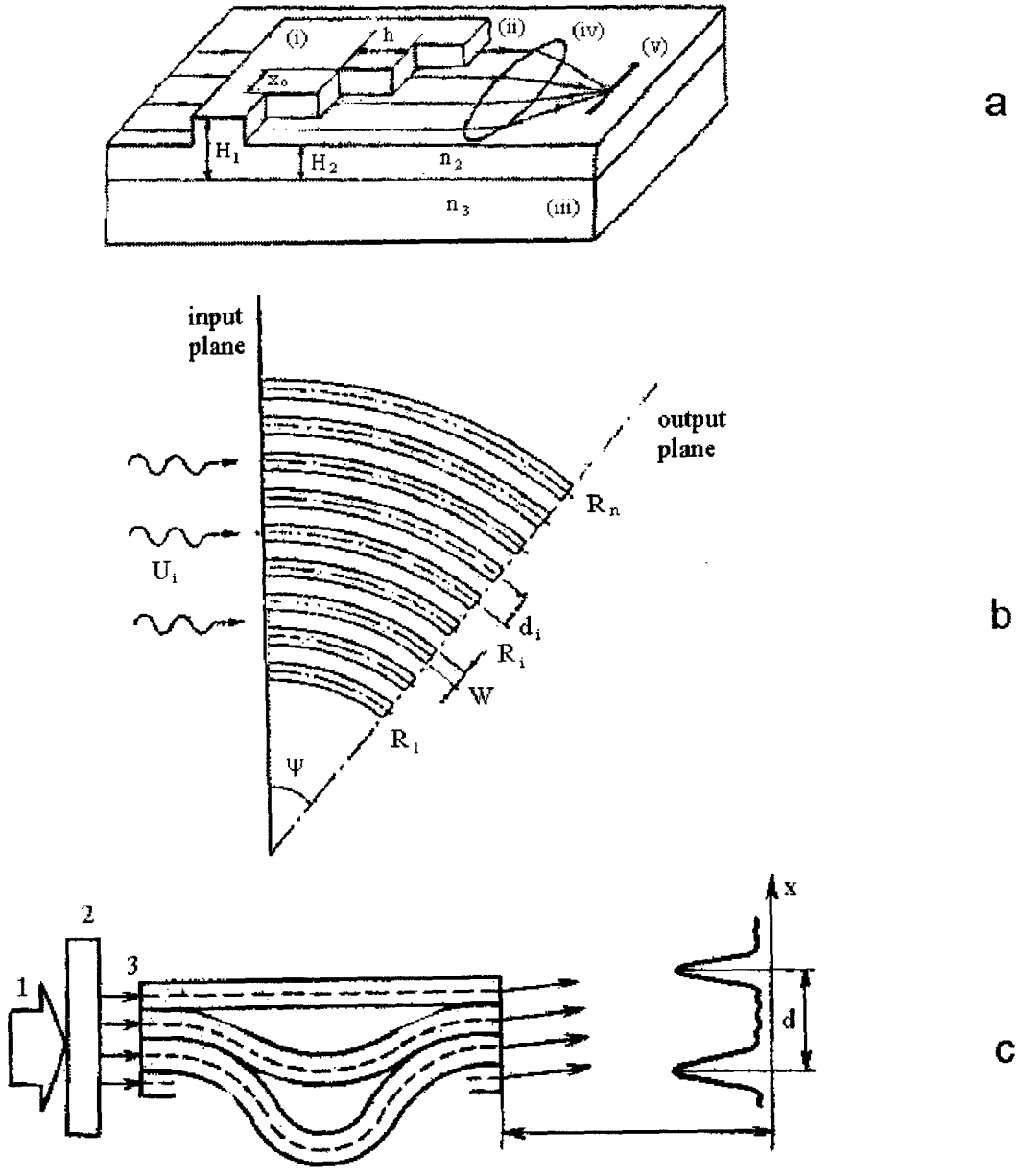

Fig. 1. Schemes of disperse systems: transparent WSA (a), WDM based on channeling waveguides (b), and WSA based on fiber-optics waveguides (c). (a): i) and ii) thin-film waveguides, iii) quartz substrate, iv) planar lens, and v) devices for recieving optical signals; (c): 1) laser, 2) planar lens, and 3) fibers.

should be taken into account, i.e., $\Delta\gamma$ should be replaced by 2γ. In all the above cases, the expression for the dispersion factor is found to be more complicated than that for a bulk Michelson echelon because of the waveguide propagation of radiation. For a WSA (Fig. 1a) [11], we have

$$b = \Delta\gamma - \lambda\frac{\partial\Delta\gamma}{\partial\lambda} - \lambda\sum_j \frac{\partial\Delta\gamma}{\partial n_j}\frac{\partial n_j}{\partial\lambda}, \tag{2}$$

where n_j are the refractive indices of the waveguides' media. The second and third terms on the right-hand side of (2) are determined by the waveguide dispersion and the material dispersion of the waveguides' media with allowance made for a fraction of radiation propagating in each medium. Analysis of the dependences of the dispersion factor on γ_1, γ_2, and $\Delta\gamma$ [11] showed that the terms appearing in (2) can be both negative and positive and the value of b can exceed $\Delta\gamma$ several times.

The schemes shown in Fig. 1 can be fabricated either in hybrid or in waveguide versions. In the former case, optical signals $\lambda_1, \ldots, \lambda_n$ are introduced into the carrier waveguide and then into the dispersive system either with the use of a lens and a coupling prism or directly from a FO waveguide with the use of a waveguide lens. The spectrum of the received signal is observed at the exit of the dispersive system in the focal plane of the output lens. On the basis of theoretical studies reported in [6–9], the corresponding models with specified calculated parameters were constructed, and consistent results were obtained. In particular, longitudinal modes produced in a He–Ne laser and separated by 0.08 Å were resolved by using the FO spectral analyzer with a resolution of 10^6 [8].

A promising feature in the development of waveguide spectral multiplexers is the integration of dispersive and focusing components (see, e.g., [6, 9]). This integration was first suggested and implemented in [6] by forming a quadratic-phase distribution at the exit of the dispersive system; this distribution was obtained by a slight variation in the length of optical channels in the dispersive system. Focusing was observed in a planar waveguide in the focal plane of the focusing system. Later, this scheme was improved (see, e.g., [7]) and is now used with insignificant modifications in the majority of works devoted to WDM/D. In such a scheme, the input and output of the dispersive system are coupled with the use of two star couplers that act as focusing components (Fig. 2). Optical signals at fixed wavelengths $\lambda_1, \ldots, \lambda_n$ coming from the FO waveguide are fed to the input of one of the star couplers, propagate along the planar waveguide, and excite the channel waveguides of the dispersive system. The latter has a constant difference in optical path lengths between neighboring channels. Optical signal are spatially separated in wavelengths $\lambda_1, \ldots, \lambda_n$ in the second star coupler and are then focused at the output facets of FO waveguides. Thus, the input optical signals are demultiplexed. If the ray path is reverse, the system operates as a multiplexer.

The wavelengths for the TE and TM polarizations are found to be different if the waveguides exhibit birefringence, i.e., if the effective refractive indices for the TE and TM waves differ. In order to compensate for this difference, a half-wave plate (shown by the dotted line in Fig. 2) is inserted in the middle of the waveguide array. The principal optical axis of this plate is set at 45° to the waveguide surface in order to change the polarization direction of the TE wave to that of the TM wave and vice versa. Thus, the effect of polarization is completely eliminated. In spite of the fact that other methods of solving this problem have been suggested, the half-wave-plate method was preferred because it allowed one to eliminate completely the sensitivity to polarization without decreasing the waveguides' birefringence [12, 13].

3. Implementation of Wavelength-Division Multiplexers/Demultiplexers

In connection with the prospects for direct use of WDM in communication systems, the following issues become especially important:

attenuation of optical signals when they pass through the multiplexer,

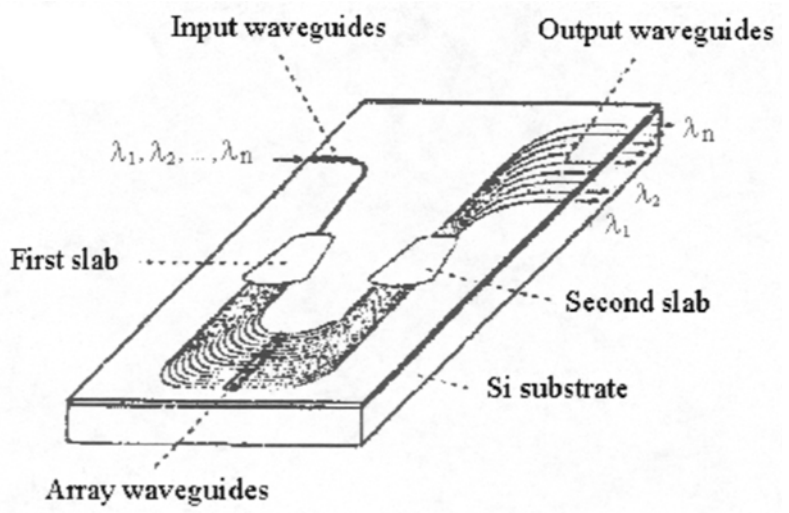

Fig. 2. Dispersive WDM system with the input and output coupled by two star couplers.

maximum number of channels,

flatness of the amplitude–frequency characteristic of the multiplexer over the channels in the entire range of wavelengths (frequencies) of the multiplexer and in a single channel,

cross-talk interferences,

insensitivity to polarization,

the cost of the system.

These issues are directly related to the materials from which the waveguides are made, to the construction of the waveguides, to the details of the circuit design, to the system's characteristics required for specific applications, and so on. Some of these issues are considered in what follows.

3.1. Wavelength-Division Multiplexers/Demultiplexers Based on SiO_2

When using multiplexers, losses in the system are of fundamental importance. The losses include those in rectilinear waveguides, in bent portions, and at connections of planar waveguides with channel waveguides and FO waveguides. Considering the losses in general, it is customary to deal separately with "on-chip" losses (i.e., in the waveguide scheme) and the losses in the fiber-to-fiber coupling. The latter losses include those at the connection of the input FO waveguide with the planar waveguide of the star coupler and those occurring in inputting the radiation from the second star coupler into the output FO waveguides (Fig. 2).

Losses in the waveguides and in the bent portions of the channel waveguides can be minimized by choosing the appropriate materials of waveguides, their parameters, and using bends with fairly large radius of curvature. The losses at the connections of the channel waveguides with the planar waveguides of star couplers can be significant. In order to reduce these losses, it was suggested to use horns and narrowing waveguides, to vary the distance between output ends of the channel waveguides, and so on. For a SiO_2/Si waveguide system, the fiber-to-fiber losses amount to 2.3–2.8 dB [14–16]. At the same time, the on-chip losses are equal to 1.7 dB [14].

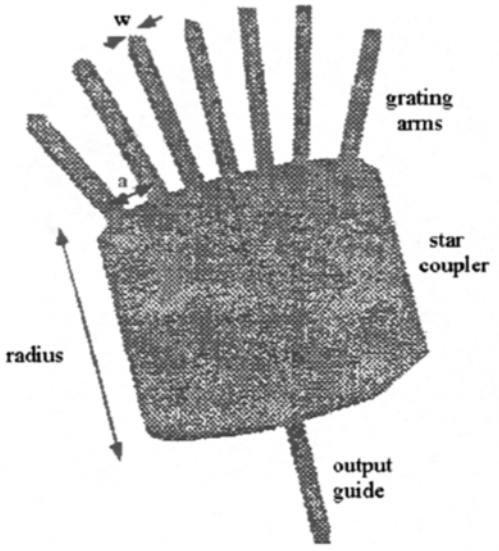

Fig. 3. Connection of the channel waveguides with the star coupler.

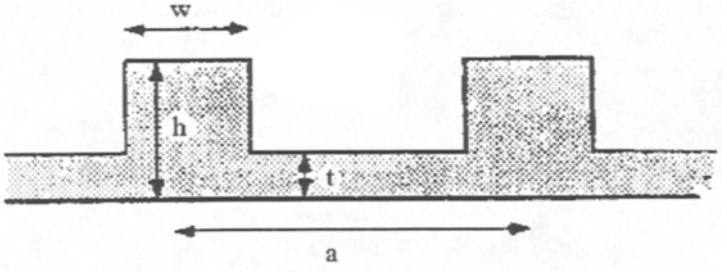

Fig. 4. Cross section of the channel waveguides shown in Fig. 3.

The losses in WDM were studied systematically using a program that accounted for radiation propagation in three-dimensional space [17, 18]. The influence of various parameters of the channel waveguides (such as the thickness of the plate, the waveguide width, the ridge height, etc.) on losses in transferring power from the channel waveguides to the star coupler was investigated. The region where channel waveguides are connected to the star coupler and the cross section of channel waveguides are illustrated in Figs. 3 and 4. To relate the fields in the channel waveguides feeding the radiation to the star-coupler region to the field at the other side of the star coupler, the Fourier transform can be used. Since all the channels are focused at a point on the other side of the star coupler and since the channels form a periodic array, it is merely required to simulate the field emitted from a separate channel. The fields formed as a result of the excitation by other channels are obtained by superposition. The procedure for calculating the fields involves the following:

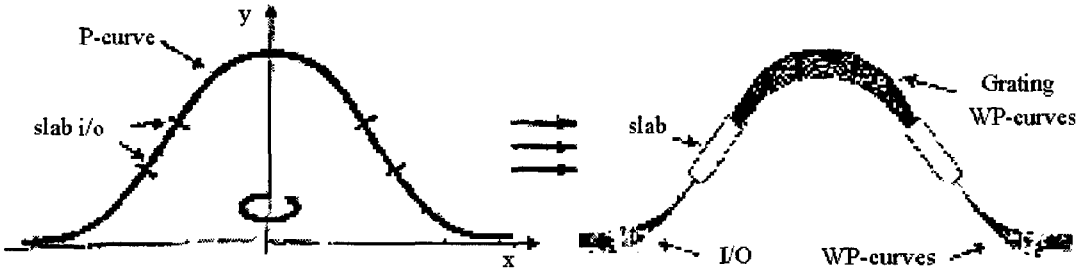

Fig. 5. Generation of a phasar from the P-curve.

The light propagation from a single waveguide channel to the end of the array is considered. Then overlapping of the fields with the waveguiding-plate modes is calculated in order to determine the fields produced by using the star coupler. After that, the fast Fourier transform is performed. As a result, the field at the other end of the star coupler is obtained.

A study of the losses showed that, in order to maximize the coefficient of transfer through the star coupler, one should use thick waveguide layers, small difference between refractive indices of the waveguiding layer and the substrate, short ridged waveguides, and large filling factors w/a. The on-chip losses can be lower than 0.2 dB for the WDM [a waveguide-grating router (WGR)] shown in Fig. 3 with the following optimum parameters of the waveguides:

thickness of waveguiding plate $t = 0.5$ μm,

height $h = 4$ μm and width $w = 7$ μm of the ridge,

distance between midlines of the channels $a = 9$ μm,

relative difference in refractive indices $\Delta n/n = 0.67\%$ with $n_{\text{substr}} = 1.4457$.

Reduction of losses in the signal propagation depends to a large extent on the appropriate choice of the optical-channels' shape. A method for solving the problem of minimizing the losses is suggested in [19] and is based on the procedure reported in [20]; this method consists in the use of a family of polynomial (P and WP) curves (Fig. 5). The latter make it possible to connect the start and end points with curves having continuously varying curvature and optimize radiation propagation along the channels with minimum losses. Thus, the minimum dimensions of the system are defined by a given level of losses. Calculations are performed using a simple algorithm on a PC. The method proposed was used to design and fabricate a multiplexer based on the SiO_2 waveguide layer deposited by gas-phase epitaxy onto silicon substrate. The parameters of this multiplexer are listed in Table 1.

The measured fiber-to-fiber losses were 5 ± 2 dB, the average spectral interval between the channels was 199.5 GHz, and the average passband of the channels measured at the half-peak intensity was 44 GHz. Within the channel's passband, the cross-talk interferences amounted to 35 dB.

As a result of the channels' coupling, aberrations appear. In order to diminish these effects, a correcting scheme can be used [21]; this scheme optimizes the location of foci of star couplers and the lengths of channels in the dispersive system in such a way as to ensure a more precise execution of the Fourier transform in the star couplers. A multiplexer described in [21] can operate as an $N \times N$ switch. If N lasers are coupled to the inputs of the multiplexer, with each of the lasers being tuned within N wavelengths, then any laser can be coupled to any output channel.

In addition to ridged waveguides, buried waveguides and waveguides coated with special layers are used. In this case, waveguides whose core had an increased refractive index due to doping, composite waveguides,

TABLE 1. Parameters of the SiO_2 Waveguide Multiplexer.

Operating wavelength	1.55 μm
Refractive index of the substrate	1.469
Difference in the refractive indices	$1.5 \cdot 10^{-2}$
Dimensions of the channel (width × total height × etched height)	6.5 × 4.5 × 2.5 μm
Number of input/output channels	16/16
Spectral resolution	16 nm (200 GHz)
Number of channels	60
Length of the dispersive component	6.1 mm
Distance between the channels at the input of the star coupler	20 μm
Interference order	60
Difference between optical path lengths in two neighboring channels	63.1 μm
Dimensions of the system	4.2 × 1.7 cm

TABLE 2. Characteristics of Channel-Waveguide Multiplexers.

Parameters	Experimental (theoretical) results			
Center wavelength λ_0 (designed value)	1.5476 μm (1.548 μm)	1.5521 μm (1.552 μm)	1.5498 μm (1.550 μm)	1.5496 μm (1.550 μm)
Spectral separation of channels $\Delta\lambda$	15 nm	2 nm	0.8 nm (100 GHz)	0.4 nm (50 GHz)
Number of channels N	8	16	32	64
Difference in the path length ΔL	12.8 μm	50.3 μm	63 μm	63 m
Slab arc length of the star coupler f	2.38 mm	5.68 mm	11.35 mm	24.2 mm
Order of interference m	12	47	59	59
Number of channels in the dispersive system	30	60	100	100
On-chip losses for λ_0	2.4 dB	2.3 dB	2.1 dB	3.1 dB
Passband at a level of −3 dB	6.3 nm (6.3 nm)	0.74 nm (0.75 nm)	40 GHz (37 GHz)	19 GHz (21 GHz)
Cross-talk interferences	< -28 dB	< -29 dB	< -28 dB	< -27 dB

and so on [9, 19, 22–24] were employed. The core of the channel waveguides has typically an area of 25–50 μm^2 and the difference in refractive indices amounts to a fraction of $0.01\,n$, which ensures that the losses in the radiation propagation along the waveguides and in the regions of waveguide connections to the FO waveguides are low (0.05–0.1 dB and ~ 0.1 dB, respectively). Table 2 lists the experimental and theoretical characteristics of multiplexers fabricated on the basis of channel waveguides with the cross-section area and the difference between the refractive indices equal to 7×7 μm and 0.75%, respectively [25].

Comparison of the theoretical and experimental results listed in Table 2 for various types of multiplexers shows that characteristics such as the center wavelength, the number of channels, the spectral interval between the channels, and the passband at a level of -3 dB can be rather accurately predicted by the ray-propagation method [25]. Thus, waveguide spectral multiplexers based on SiO_2/Si make it possible to realize low fiber-to-fiber losses and integrate the optical and electronic circuits on the basis of Si.

Progress in the field of development of low-loss SiO_2/Si waveguides and WDM/D based on them made it possible to fabricate reliable and economical modules of multiplexers for systems with spectral compression. The multiplexing 1×8 modules based on SiO_2/Si are brought up to the commercial level [26]. In the operation of a multiplexer, stabilization of the center wavelength is extremely important, which necessitates temperature control; the latter requires knowledge of the temperature dependence of the center-wavelength shift. In connection with this, the aforementioned modules were subjected to thermal tests. In this case, the multiplexer's parameters such as the shift of the center frequency with temperature and the thermal degradation were of the most interest. The tests were performed both for systems based on bare crystals and for modules encapsulated in plastic. The modules were provided with special heaters and temperature sensors (thermistors). The tested modules had the following characteristics:

induced losses < 10 dB,

interval between channels equal to 200 GHz (1.6 nm),

polarization sensitivity less than ± 0.05 nm,

effect of losses by polarization amounting to less than 1 dB at room temperature,

used power 5 W,

case dimensions $100 \times 55 \times 17$ mm.

The results of tests of encapsulated modules demonstrated that the induced losses varied insignificantly (within ± 0.5 dB) after operation for 950 h at a temperature of 85° C. The center wavelength shifted by less than 0.01 nm in the course of testing. These experimental results show that the encapsulated multiplexer modules can operate reliably and stably even at enhanced temperatures.

3.2. Wavelength-Division Multiplexers/Demultiplexers Based on InP

Until recently, WDM (phasars) based on SiO_2/Si have demonstrated the best performance and seemed to be the most suitable for practical purposes. However, substantial progress has recently been made in the development of waveguide systems based on semiconductor compounds. The latter make it possible to integrate both passive and active devices on the same substrate. Thus, multiplexers based on the deep-profiled-ridged-waveguide structure shown in Figs. 6 and 7 were fabricated [27]. The structure consists of a quaternary InGaAsP layer (1 μm thick) and an upper InP layer (1 μm thick), which were grown by molecular-beam epitaxy from gaseous sources. The waveguide, 2.5 μm thick, was deeply etched (by ~ 0.6 μm) below the carrier layer by multistep reactive-ion etching [28] in order to remove the polymer from the ridge sides and to obtain vertical side walls. The structure's parameters were designed for obtaining the same propagation constants for the TE and TM polarizations. The advantage of a structure with deep etching consists in the fact that the birefringence is independent of the depth of etching; rather, it is defined solely by the thickness of the waveguiding layer and by the waveguide width. Another advantage of this structure is the high degree

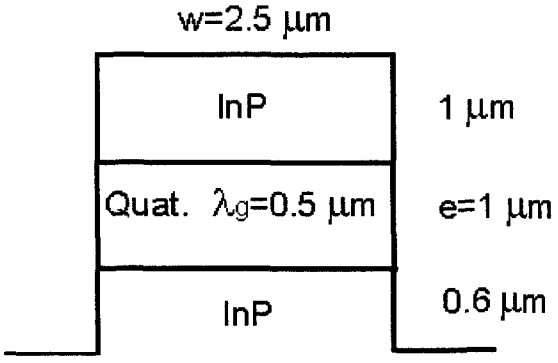

Fig. 6. A deep-profiled ridged (nonbirefringent) waveguide structure.

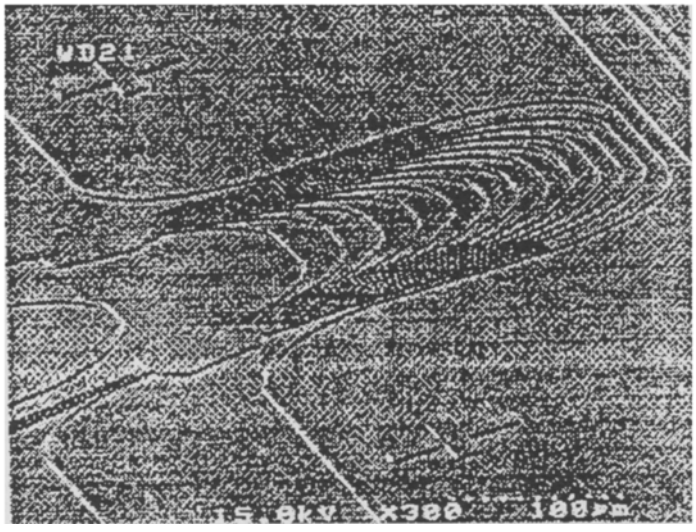

Fig. 7. SEM photograph of the demultiplexer based on a deep-profiled ridged waveguide structure.

of optical confinement, which makes it possible to use bends with small radius of curvature ($R \sim 70$ μm) without a significant increase in the losses. Thus, very small-sized multiplexers can be fabricated.

Measurements performed for two polarization-insensitive phasars with 4 and 16 channels in the region of 1.55 μm and with dimensions of 0.5 × 0.5 mm and 1.0 × 0.9 mm, respectively, yielded the following characteristics:

intervals between neighboring channels 3.2 and 2.03 nm,

cross-talk interferences 28 and 20 dB,

induced losses 11 and 13 dB.

These results indicate that the above multiplexers are suitable for monolithic integration with active devices, such as diode lasers, amplifiers, detectors, and so on.

4. Integration of Optical Devices

The prospects of using the WDM/D in the end stations of FO communication systems are directly related to the possibility of their integration with the radiation sources, detectors, amplifiers, and so on.

4.1. Integrated Sources of Radiation

In the transmitting stations, the radiation coming from an array of lasers operating at the wavelengths $\lambda_1, \ldots, \lambda_n$ should be combined and introduced into a single channel in order to be inputted in the FO waveguide of the optical communication line. This can be accomplished by using a Y-coupler array, by combining the laser radiation with the use of an WDM, by integrating the amplifiers and WDM into a single unit with a single output channel, and by other methods [29–31].

Combiners based on InP [31] were integrated on the same substrate with an array of four lasers with distributed feedback (DFB) and wavelength 1.55 μm; the spectral interval between individual emitters is equal to 2 nm. In this case, the induced losses were significant. Later, the losses were somewhat reduced. Previously, a similar system consisting of six DFB lasers was reported in [29]. Figure 8 illustrates an integrated scheme of a module that involves four DFB lasers integrated with a polymeric power 1×4 combiner fabricated on the same InP substrate. A photograph of the cross section of a polymer buried structure is shown in Fig. 9. The module was fabricated in two stages. The first stage consisted in fabrication of a laser structure with buried ridged waveguides by molecular-beam epitaxy and by etching with a reactive-ion beam. A junction between the active and passive regions was accomplished by vertical etching down to the substrate with the use of a $CH_4/H_2/Ar$ mixture. The second stage of fabrication of the module consisted in the formation of a passive combiner based on a polysulfone waveguide as a waveguide layer and of PMMA framing layers. Polymeric layers were deposited onto the InP substrate with the use of a centrifuge, and the stripe waveguides of the combiner were then formed by photolithography and reactive-ion etching [32].

Similar modules were fabricated using arrays of lasers with a distributed Bragg reflector (DBR) [33] (Fig. 10). As distinct from the DFB lasers operating at a fixed wavelength determined by the period of the Bragg structure, the DBR lasers make it possible to tune the wavelength more flexibly by varying the current in the passive section of the Bragg reflector. Thus, an increase in current from 0 to 30 mA resulted in a variation in the laser wavelength by 4.5 nm. Four DBR lasers operated in the wavelength region of 1.55 μm, with the spectral interval between their wavelengths being 4 nm. The active-region length of the lasers was about 0.900 mm, and the Bragg-reflector section was 0.5 mm in length. By varying the current in the Bragg reflector, it was possible to tune the laser wavelength to an accuracy higher than ± 0.2 nm. The WDM was fabricated using three stages of growth by metal-organic vapor-phase epitaxy (MOVPE). Initially, an active layer composed of four GaInAsP strained potential wells with an optical confinement was formed. Laser active regions were subjected to dry etching, and a passive semiconductor layer having a bandgap of 1.3 μm was obtained by selective epitaxial growth, in the course of which a silicon nitride mask was used. As a result, a structure composed of active and passive regions (facet-to-facet connected) was realized [34]. A structure composed of a quaternary-compound thin layer inserted between the InP layers in order to be able to select precisely the grating's thickness was grown on the upper surface of the passive layer. Four gratings with differing periods were then fabricated with the use of one-dimensional holographic lithography [35]. The first grating had a period of 240 nm, and the periods of other gratings differed by 0.625 nm, which ensured a spectral interval between the emission wavelength of the laser of 4 nm. Ridged waveguides of Y splitters in the combiner and the laser waveguides were fabricated in a single lithography process. The measured power of each laser was 0.2 mW. The dimensions of the device constructed were 3×1 mm.

In order to build optical networks with WDM/D, it is expedient to use radiation sources that generate simultaneously a number of frequencies with stable and strictly controlled spectral intervals between these

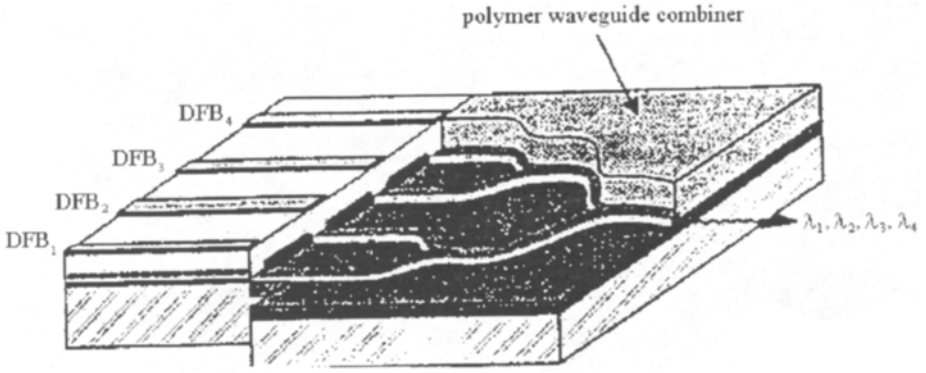

Fig. 8. Schematic diagramm of the integrated device. Overall dimensions of the chip are 1.2 × 0.5 mm.

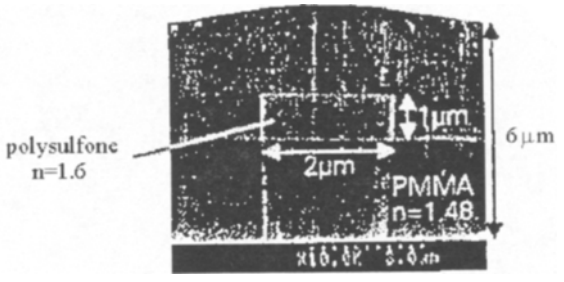

Fig. 9. A photograph of cross section of the buried polymer waveguide structure.

frequencies. The multifrequency lasers are such sources [36]. These lasers (Fig. 11) are, in fact, amplifiers with cleaved mirror facets, which (together with a single output port) form an optical cavity. If the amplifiers ensure a gain sufficiently high to compensate for all the losses in the cavity, lasing occurs at the wavelength defined by the filter in the corresponding channel. Thus, each of K amplifiers in the ports from 1 to N would emit the optical wavelength λ_k. Intervals between optical channels are defined to a high accuracy by the internal resonator. Simultaneous operation at all wavelengths is achieved by a simple switching-on of all amplifiers. Specific information for each optical channel at λ_k is provided by direct modulation of the bias current of the corresponding amplifier. The operation of a multifrequency laser involving 16 channels was demonstrated. The system can provide a power of 13 dB/m per channel in the case where the signal is inputted in a single-mode fiber and all the channels are operating simultaneously. Each channel can be modulated to a rate of 622 Mb/s, demonstrating thus a total bit rate of 10 Gb/s (16 × 622 Mb/s). The measured average interval between channels was 200 GHz. The direct modulation rate was limited as a result

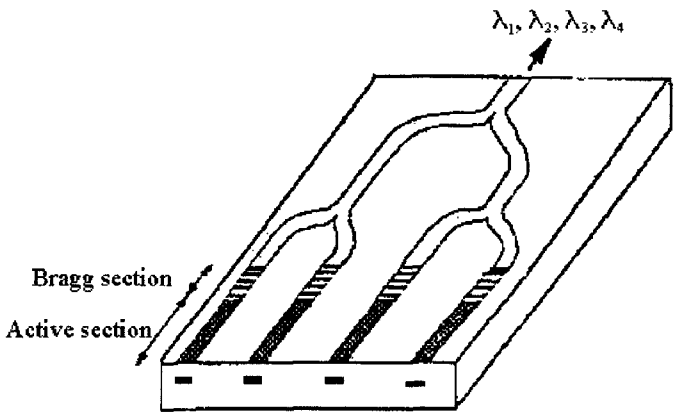

Fig. 10. Photonic integrated circuit which includes an array of four DBR lasers monolithically integrated with a coupler.

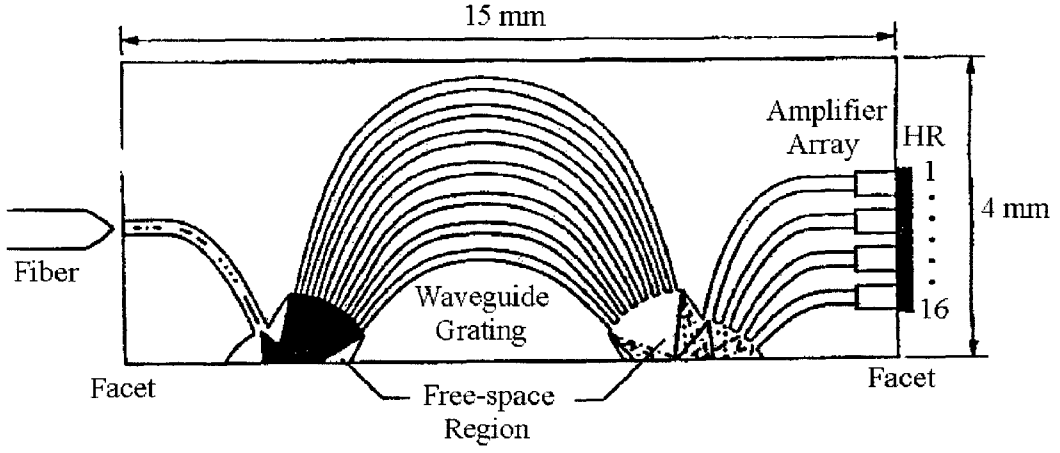

Fig. 11. A multifrequency laser with cleaved mirror facets for networks with WDM/D.

of delay related to the time of a single pass through the cavity and was equal to 2.5 GHz. If the system's size is reduced, a higher modulation rate can be attained.

A comparison of mutifrequency lasers with the DFB-laser array made it possible to assess the advantages and disadvantages of both systems. Thus, each individual DFB laser can be modulated with a very high rate because it has a short cavity. In addition, the size of a DFB laser chip is much smaller than that of a mutifrequency laser because, in the former case, there is neither focusing grating nor waveguide array grating. However, an advantage of multifrequency lasers consists in the fact that they make it possible to obtain spectral channels located to a high accuracy determined by the use of an independent filter for each

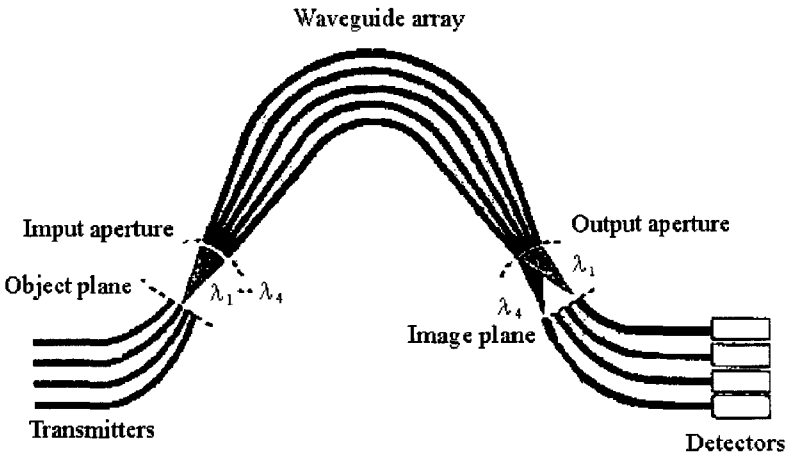

Fig. 12. Schematic representation of a dispersive waveguide system integrated with photodetectors.

emitted wavelength [37]. As distinct from multifrequency lasers, the individual wavelengths of DFB lasers can be shifted with respect to each other as a result of degradation. In addition to these disadvantages of the DFB laser array, it may be noted that the internal losses of this array are proportional to the number of channels; therefore, an increase in this number is undesirable. As a result of the above comparison, we can draw the following conclusions: if a small number of channels is needed, the DFB lasers are superior owing to their compact size. However, if the number of channels with different wavelengths increases, the possibility to control the position of optical channels in spectral intervals, which is inherent in multifrequency lasers, can overcome the disadvantages related to their size. Thus, a multifrequency laser may find use in systems with a waveguide spectral compression, which require a large number of channels with different wavelengths but with a moderate rate of data flow in each channel.

4.2. Integration of Wavelength-Division Multiplexers/Demultiplexers and Photodetectors

Integration of photodetectors based on InP with demultiplexers based on conventional (nonwaveguide) concave reflecting gratings and transmission gratings was reported in a number of publications [38–40]. A technology that is more sophisticated with respect to integration of demultiplexers with photodetectors was demonstrated on the basis of SiO_2 [25, 41, 42] and also InP [43, 44] waveguides. A four-channel demultiplexer having low losses was integrated monolithically to the photodetectors [44]. The demultiplexer consisted of a dispersive waveguide system connected with planar focusing regions (Fig. 12). Ridged waveguides with a transverse difference in refractive indices equal to 0.037 and $n_{\text{eff}} = 3.29$ (for the TE polarization) were used in the system. The width and height of the ridge were 2 and 0.35 μm, respectively. Light from the output waveguides was fed to photodetectors via a coupler system using the penetrating field. The layer structure was optimized with the aim of increasing the absorption of the photodetector. This structure was grown by MOVPE on the n^+-InP substrate [45] and included the following layers:

an undoped buffer InP layer 1.5 μm thick,

an undoped waveguiding InGaAs layer ($\lambda_{\text{gap}} = 1.3$ μm) 0.6 μm thick,

an undoped upper framing waveguide layer 0.3 μm thick,

an absorbing n-InGaAs ($1 \cdot 10^{17}$ cm^{-3}) 0.27-μm layer,

a nonwaveguiding contact p-InGaAs ($2 \cdot 10^{18}$ cm^{-3}) layer 0.2 μm thick.

The photodetector has dimensions 150×80 μm. The internal quantum yield was higher than 90%. Outside of the photodetector, a layer structure containing thin waveguide layers was grown.

The multiplexer's characteristics were measured with the use of a tuned laser. The measured interval between channels was 1.8 nm. The overall channel passband at the level of 0.5 was 0.7 nm. The demultiplexer integrated monolithically with photodetectors featured losses equal to 3–4 dB for TE polarization and losses higher by 0.5 dB for TM polarization. The external sensitivity of the photodetector was 0.12 A/W. The overall external losses including the losses in the coupling between the photodetector and the waveguide were 10 dB, and the cross-talk interferences amounted to 12–21 dB. The system, the photodetectors and the input stripe waveguides included, has dimensions 3.0×2.3 mm.

4.3. Optical Multiplexers with Adding and Dropping of Channels

An optical multiplexer with adding and dropping of channels [an add/drop multiplexer (A/DM)] is a device that provides simultaneous access to all channels at corresponding wavelengths in WDM/D-based communication lines [46–48]. Figure 13 shows the configuration of such a waveguide 16-channel optical multiplexer [47]. It involves four WDM/D and 16 double-gate thermo-optical (TO) switches. Four WDM/D having identical parameters are positioned at the site where their planar focal regions intersect. In the range around 1.55 μm, spectral intervals between channels and the dispersion region were 100 GHz and 3300 GHz (26.4 nm), respectively. The signals $\lambda_1, \lambda_2, \ldots, \lambda_{16}$ coming from the multiplexer and having identical spectral intervals between them are connected to the main input ports (add ports). These 16 signals are separated with the use of WDM/D_1 (WDM/D_2) and are fed to the left-hand branches (right-hand branches) of TO switches. Any optical signal fed to a two-way TO switch comes through the cross port of either of four Mach–Zehnder interferometers before arriving at the output port. On the other hand, any signal with a certain wavelength can be dropped from the main output port and directed to the branching port by changing the corresponding condition in the switch. A signal with the same amplitude as the branched one can be added to the main output port if it is connected to the add port (see Fig. 13). For example, if the TO switches SW_2, SW_4, SW_6, SW_7, SW_9, SW_{12}, SW_{13}, and SW_{15} are in the position "ON," the separated signals λ_2, λ_4, λ_6, λ_7, λ_9, λ_{12}, λ_{13}, and λ_{15} are dropped from the main output port (the solid line) and are connected to the drop port (the dashed line) as shown in Fig. 14. The cross-talk interferences for the positions "ON"–"OFF" were less than 28.4 dB, with on-chip losses amounted to 8–10 dB. The above-described add/drop multiplexers are very promising for all communication lines incorporating WDM/D and enable the optical network to be transparent for signals with high bit rates and large formats.

The outlook for wide practical application of A/DM has motivated researchers to develop tools for designing complex photonic integrated networks. For a four-channel A/DM, it was suggested to initiate design at the symbolic level and, starting from this level, perform a simulation and masking of the breadboard [49]. The system of computer-aided design (CAD) used was based on the known specialized system for design in the microwave range [50].

Simulation of a phasar was performed in two stages. Initially, a phasar configuration with the desired specifications (including the number of input and output ports, the center wavelength, and the spectral interval between channels) was devised. Then wave propagation through the phasar was simulated.

The design of the phasar configuration was based on the description given by Smit [7] and included two star couplers connected by array rectilinear and bent waveguides. A phasar having N input and M output waveguides was described by $(N+M) \times (N+M)$ S-matrices. The elements of the matrix S_{ij} were calculated in the following manner. First, the field emitted by the port i and the coupling coefficients for each waveguide of the array were calculated by the method reported in [51, 52]. Then, the wave propagation in each waveguide

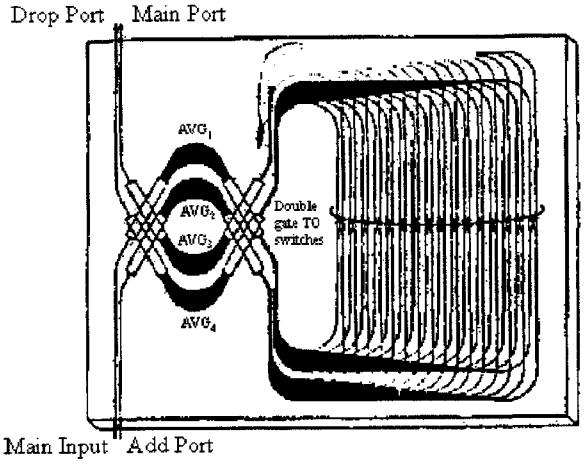

Fig. 13. Waveguide configuration of a 16-channel add/drop optical multiplexer with double-gate TO switches.

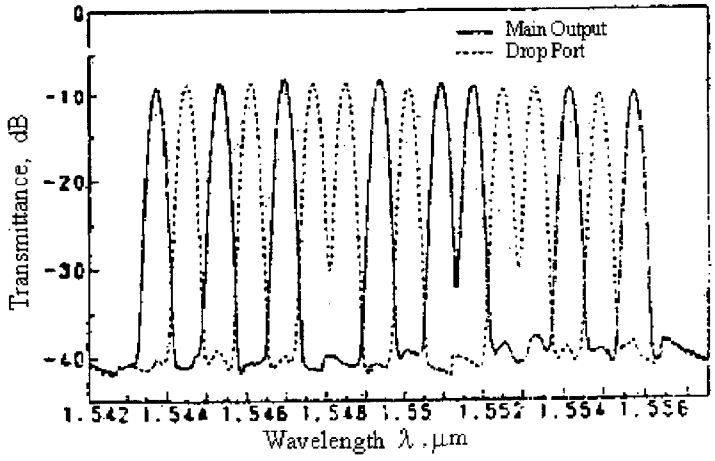

Fig. 14. Transmission spectra from the main input port to the main output and drop ports in the 16-channel A/DM (TO switches SW_2, SW_4, SW_6, SW_7, SW_{12}, SW_{13}, and SW_{15} are in position "ON").

taking into account losses in the connections and radiation losses in the bent waveguides was calculated. Finally, the coefficients of coupling between each waveguide in the array and the output waveguide j were calculated by the same method as was used in the case of input ports.

A symbolic representation of the 6×6 phasar array along with the mask scheme is shown in Fig. 15. In the next stage, a model of A/DM was designed. This multiplexer is composed of a 6×6 phasar and reverse waveguide loops. The latter incorporate switches of the Mach–Zehnder-interferometer type that open and

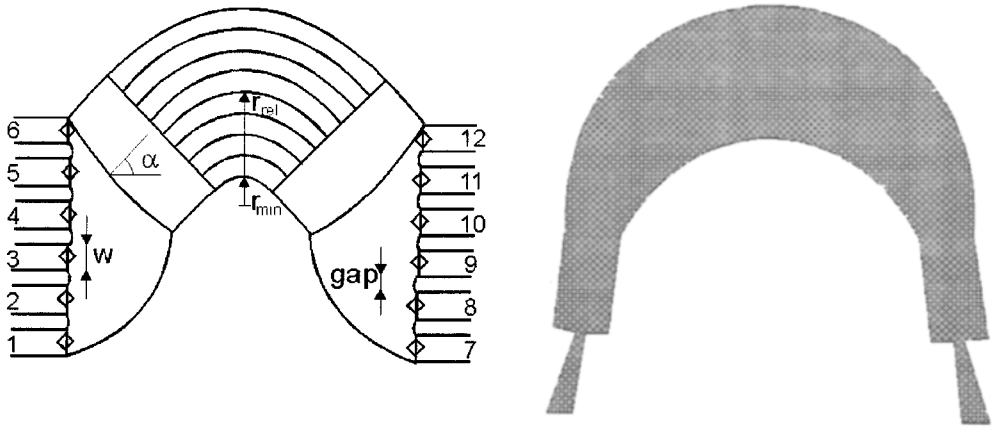

Fig. 15. Symbolic representation of a 6 × 6 phasar and a mask scheme.

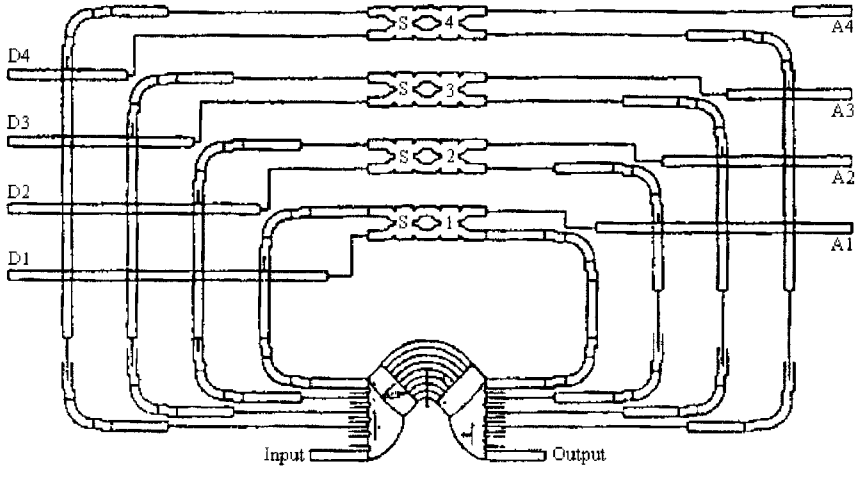

Fig. 16. Symbolic representation of a four-channel A/DM curcuit.

close the loops. A symbolic representation of A/DM is shown in Fig. 16.

A four-channel A/DM constructed identically to the design was implemented based on InP [53]. Comparison of the results of simulation with those of measurements showed that the maximum of the passband of an individual channel was shifted by 9 nm. This was largely due to the difference between the designed and fabricated waveguide structures. The measured losses amounted to 7–9 dB, and the residual signal in the bandwidth of the neighboring channel was ~30 dB lower in amplitude than the input signal. These values are in fair agreement with the results of calculations.

5. Conclusions

Waveguide spectral multiplexers/demultiplexers are the key to solving the problem of using the entire extremely wide passband of fiber-optics waveguides. The most developed are WDM/D based on SiO_2/Si and InP. The former feature lower on-chip losses, while the passive semiconductor (integrated optics) circuits can be directly integrated to the radiation sources, amplifiers, photodetectors, and the like. Furthermore, optical and electronic components can be combined on the same substrate. Optical WDM systems with dense arrangement of channels with different wavelengths are fabricated by standard (high-quality) lithography. Connections of optical planar integrated circuits to fiber-optics waveguides are well developed and do not introduce significant losses. The dimensions of devices (without encapsulation) do not exceed 1–2 cm^2. Such characteristics will lead to rapid development of a new generation of inexpensive and commercially viable devices not only for long-range communication systems but for local wide-band communication systems of the building-to-building type as well.

References

1. E. M. Dianov and A. A. Kuznetsov, *Kvantovaya Élektron.*, **10**, 245 (1983).
2. V. A. Sychugov and V. G. Elenskii, *Zarubezhn. Radioélektron.*, No. 12, 50 (1983).
3. L. N. Deryugin, I. V. Tcheremiskin, and T. K. Chekhlova, "Multiray interferometers based on ring cavities," in: *Abstracts of Papers Presented at XI All-Union Conf. on Coherent and Nonlinear Optics* [in Russian], Yerevan (1982), Part II, p. 454.
4. L. N. Deryugin, A. I. Gudzenko, I. V. Tcheremiskin, et al., "Spectrum analyzer and technology of its production," USSR Inventor's Certificate No. 1204011 (September 8, 1985).
5. A. I. Gudzenko, I. V. Tcheremiskin, and T. K. Chekhlova, *Izv. Vyssh. Uchebn. Zaved., Radioelektronika*, **31**, 77 (1988).
6. M. K. Smit, *Electron. Lett.*, **24**, 385 (1988).
7. M. K. Smit, "Integrated optics in silicon-based aluminum oxide," *PhD Thesis*, Delft University of Technology, Delft, The Netherlands (1991).
8. Kh. G. Vaskes, I. V. Tcheremiskin, and T. K. Chekhlova, *Kvantovaya Élektron.*, **19**, 387 (1992).
9. H. Takahashi, S. Suzuki, K. Kato, and I. Nishi, *Electron. Lett.*, **26**, 87 (1990).
10. A. A. Shishlovskii, *Applied Physical Optics* [in Russian], Fizmatgiz, Moscow (1961).
11. I. V. Tcheremiskin, T. K. Chekhlova, and A. G. Timakin, *Electron. Lett.*, **26**, 1952 (1997).
12. H. Takahashi, K. Oda, H. Toba, and Y. Inoue, *J. Lightwave Technol.*, **13**, 447 (1995).
13. H. Takahashi, Y. Hibino, and I. Nishi, *Opt. Lett.*, **17**, 499 (1992).
14. C. Dragon, C. A. Edwards, and R. C. Kistler, *IEEE Photon Technol. Lett.*, **3**, 896 (1991).
15. P. C. Clemens, G. Heise, R. Marz, et al., *IEEE Photon Technol. Lett.*, **7**, 1040 (1995).
16. K. Okamoto, M. Ishii, Y. Hibino, et al., *Electron. Lett.*, **31**, 1464 (1995).
17. J. C. Chen and C. Dragon, "Low transition losses in waveguide grating routers," in: *Proceedings of the 8th European Conference on Integrated Optics, ECIO-97* (April 1997, Stockholm), Royal Institute of Technology, Stockholm (1997), p. 34.
18. W. P. Huang, C. L. Xu, S. T. Chi, et al., *J. Lightwave Technol.*, **10**, 295 (1992).
19. V. Delisle, G. Grand, A. Fourniez, and P. Mottier, "Reduced-size low-crosstalk PECVD silica phasar using widened continuous bends," in: *Proceedings of the 8th European Conference on Integrated Optics, ECIO-97* (April 1997, Stockholm), Royal Institute of Technology, Stockholm (1997), p. 72.
20. F. Ladouceur and P. Labeye, *J. Lightwave Technol.*, **13**, 481 (1995).
21. C. Dragon, *IEEE Photon Technol. Lett.*, **3**, 812 (1991).

22. M. Kawachi, M. Yasi, and T. Edahiro, *Electron. Lett.*, **19**, 583 (1983).
23. M. Kawachi, *Opt. Quantum Electron.*, **22**, 391 (1990).
24. S. Suzuki, Y. Inone, and Y. Ohimori, *Electron. Lett.*, **30**, 642 (1994).
25. K. Okamoto, H. Okazaki, Y. Ohimori, and K. Kato, *IEEE Photonics Technol. Lett.*, **4**, 1032 (1992); K. Okamoto, K. Moriwaki, and S. Suzuki, *Electron. Lett.*, **31**, 184 (1995).
26. S. Kobayashi, K. Schmidt, M. Dixon, et al., "High operation temperature 1×8 AWG modules for dense WDM application," in: *Proceedings of the 8th European Conference on Integrated Optics, ECIO-97* (April 1997, Stockholm), Royal Institute of Technology, Stockholm (1997), p. 80.
27. R. Mestric, M. Renaud, B. Martin, and F. Gaborit, "Up to channel phased-array wavelength demultiplexers on InP with -20 dB cresstalk," in: *Proceedings of the 8th European Conference on Integrated Optics, ECIO-97* (April 1997, Stockholm), Royal Institute of Technology, Stockholm (1997), p. 264.
28. Y. S. Oei, L. H. Spiekman, F. H. Groen, et al., "Novel RIE process for high-quality InP-based waveguide structures," in: *Proceedings of the 7th European Conference on Integrated Optics, ECIO-95* (April 1995, Delft, The Netherlands), Delft University of Technology, Delft, The Netherlands (1995), p. 205.
29. K. Aiki, M. Nakamura, and J. Umeda, *Appl. Phys. Lett.*, **29**, 506 (1976); *IEEE J. Quantum Electron.*, **13**, 220 (1977); see also R. G. Hunsperger, *Integrated Optics: Theory and Applications*, Springer, Berlin (1984).
30. U. Koren, T. L. Kock, B. I. Mîller, et al., *Appl. Phys. Lett.*, **54**, 2056 (1989).
31. N. Bouadma, R. Levenson, P. Win, et al., "Monolithic integrated four DFB lasers array with polymer-based combiner for WDM lightwave systems," in: *Proceedings of the 8th European Conference on Integrated Optics, ECIO-97* (April 1997, Stockholm), Royal Institute of Technology, Stockholm (1997), p. 126.
32. N. Bouadma, J. Liang, R. Levenson, et al., *IEEE Photon. Technol. Lett.*, **6**, 1188 (1994).
33. A. Talneau, M. Allovon, N. Bouadma, et al., "Accurate wavelength spacing and fast switching in a four channel integrated source emitting at 1.55 μm," in: *Proceedings of the 8th European Conference on Integrated Optics, ECIO-97* (April 1997, Stockholm), Royal Institute of Technology, Stockholm (1997), p. 122.
34. F. Delorme, S. Slempkes, G. Alibert, et al., *Electron. Lett.*, **31**, 1244 (1995).
35. A. Talneau, J. P. Chandonineau, J. Charil, and A. Ongazzaden, *Photon Technol. Lett.*, **7**, 721 (1995).
36. M. Zirngibl, "Multifrequency laser for dense WDM applications," *Proceedings of the 8th European Conference on Integrated Optics, ECIO-97 (April 1997, Stockholm)*, Royal Institute of Technology, Stockholm (1997), p. 254.
37. C. E. Zah, M. R. Amersfoort, B. Pathak, et al., *IEEE Photon. Technol. Lett.*, **8**, 864 (1996).
38. J. B. Soole, A. Scherer, Y. Silberberg, et al., *Electron. Lett.*, **29**, 558 (1993).
39. C. Cremer, N. Emeis, M. Schier, et al., *IEE Proc. J.*, **140**, 7174 (1993).
40. G. H. B. Thompson, S. M. Ohja, S. Clements, et al., "Fabrication of a low loss integrated InGaAsP/InP demultiplexer using $CH_4/H_2/O_2$ reactive ion etching," in: *Proceedings of the 6th European Conference on Integrated Optics, ECIO-97* (April 1993, Neuchatel, Switzerland), p. 2/12.
41. A. R. Vellekoop and M. K. Smit, *J. Lightwave Technol.*, **9**, 310 (1991).
42. H. Takahashi, I. Nishi, and Y. Hibino, *Electron. Lett.*, **28**, 380 (1992).
43. M. Zirngibl, C. Dragon, and C. H. Joyner, *IEEE Photon. Technol. Lett.*, **4**, 1250 (1992).
44. M. R. Amersfoort, C. R. de Boer, B. H. Verbeek, et al., *IEEE Photon. Technol. Lett.*, **6**, 62 (1994).
45. I. Moerman, G. Gondenys, P. Demeester, et al., *J. Cryst. Growth*, **107**, 175 (1991).
46. K. Okamoto, M. Okuno, A. Himeno, and Y. Ohmori, *Electron. Lett.*, **32**, 1471 (1996).
47. K. Okamoto, "Integrated optical WDM devices," in: *Proceedings of the 8th European Conference on Integrated Optics, ECIO-97* (April 1997, Stockholm), Royal Institute of Technology, Stockholm (1997), p. 62.

48. K. Okamoto, *Proceedings of OFC'95 (San Diego, 1995)*, p. ThB1.
49. P. Le Lourec, X. J. M. Leijtens, C. G. M. Vreeburg, et al., "*S*-matrix oriented simulation of a looped-back four channel add-drop multiplexer," in: *Proceedings of the 8th European Conference on Integrated Optics, ECIO-97* (April 1997, Stockholm), Royal Institute of Technology, Stockholm (1997), p. 18.
50. X. Leijtens, L. Spiekman, C. van Dam, et al., "CAD-tool for integrated optics," in: *Proceedings of the 7th European Conference on Integrated Optics, ECIO-95* (April 1995, Delft, The Netherlands), Delft University of Technology, Delft, The Netherlands (1995), p. 463.
51. M. Born and E. Wolf, *Principles of Optics*, Pergamon Press, Oxford (1993).
52. K. S. Chiang, *J. Lightwave Technol.*, **9**, 62 (1991).
53. C. Vreeburg, T. Uitterdijk, Y. Oei, et al., *IEEE Photon. Technol. Lett.*, **9** 191 (1997).